Clinical Radiology 74 (2019) 410.e1–410.e9

Contents lists available at ScienceDirect

Clinical Radiology

journal homepage: www.clinicalradiologyonline.net

Comparison of cardiac MRI with PET for assessment of myocardial viability in patients with coronary chronic total occlusion

J.N. Li [a], Y. He [b,*], W. Dong [c], L.J. Zhang [b], H.Z. Mi [c], D.F. Zhang [a], R.C. Huang [d], X.T. Song [a]

[a] Department of Cardiology, Beijing Anzhen Hospital, Capital Medical University, Beijing, China
[b] Department of Radiology, Beijing Anzhen Hospital, Capital Medical University, Beijing, China
[c] Department of Nuclear Medicine, Beijing Anzhen Hospital, Capital Medical University, Beijing, China
[d] Department of Cardiology, The First Affiliated Hospital of Dalian Medical University, Dalian, China

ARTICLE INFORMATION

Article history:
Received 6 May 2018
Accepted 24 January 2019

AIM: To compare cardiac magnetic resonance imaging (MRI) and positron-emission tomography (PET) assessment of myocardial viability in patients with coronary chronic total occlusion (CTO).

MATERIALS AND METHODS: Eighty patients with coronary CTO underwent cardiac MRI and PET. Cardiac MRI images were analysed using a 17-segment model, and late gadolinium enhancement (LGE) and wall motion were scored. PET was used to classify myocardial viability via myocardial perfusion and 18F-fluorodeoxyglucose, digital superscript uptake.

RESULTS: With PET as the reference standard, the sensitivity of cardiac MRI in detecting myocardial viability was 95.3%, specificity was 87.5%, positive predictive value was 96.8%, negative predictive value was 84.2%, and accuracy was 93.8% on a per patient basis. The receiver operator characteristic curve was used to analyse the performance of cardiac MRI in the detection of myocardial viability on a per-patient basis and the area under the curve was 0.910 (95% confidence interval 0.805 to 1). Cardiac MRI had the highest sensitivity and specificity for differentiating viable and non-viable myocardium as defined by PET when the cut-off value of LGE was 50%. The motion consistency and correlation of cardiac MRI and PET were analysed and kappa was 0.788 (r=0.825; p<0.001).

CONCLUSION: Compared with PET, cardiac MRI assessment of myocardial viability in patients with coronary CTO has high sensitivity, specificity, and accuracy. Therefore, cardiac MRI can be used as an important method for evaluating myocardial viability in coronary CTO patients.

Introduction

Coronary chronic total occlusion (CTO) is caused by atherosclerotic plaque rupture leading to thrombosis, thrombus regeneration leading to complete occlusion of the

* Guarantor and correspondent: Y. He, Department of Radiology, Beijing Anzhen Hospital, Capital Medical University, 2 Anzhen Road, Chao Yang District, Beijing 100029, China. Tel.: +86 15611112775.
E-mail address: heyi139@sina.com (Y. He).

https://doi.org/10.1016/j.crad.2019.01.021
0009-9260/

coronary artery with an occlusion time of >3 months.[1–3] CTO lesions are found on coronary angiography in 20–30% of patients.[4] The success rate of interventional treatment of CTO lesions is low and the postoperative complications and the requirements for the operators are high.[5] CTO lesions are even called "the last bastion" in the field of coronary artery interventional therapy.

The American College of Cardiology (ACC)/American Heart Association (AHA) and European Society of Cardiology (ESC) guidelines demonstrate the importance of myocardial viability analysis in patients with coronary CTO.[6,7] The presence or absence and the degree of myocardial viability are important in determining whether patients will benefit from interventional treatment of CTO lesions.

Nowadays, positron-emission tomography (PET) is the reference standard for evaluating myocardial viability and cardiac magnetic resonance imaging (MRI) is one of the most commonly used methods for evaluating myocardial viability[8]; however, there are few studies comparing cardiac MRI and PET assessment of myocardial viability[9–12] in particular in patients with coronary CTO. Therefore, the purpose of the present study was to compare cardiac MRI and PET assessment of myocardial viability in patients with coronary CTO.

Materials and methods

Patients

A total of 80 consecutive patients with coronary CTO confirmed by invasive coronary angiography (ICA) were recruited and studied from January 2016 to December 2017. All patients scheduled for myocardial viability assessment were scanned with both cardiac MRI and PET within 1 week of each other. All patients remained stable throughout the examination period. This study excluded patients with left main coronary stenosis >50%, acute coronary syndrome within 90 days, and decompensated heart failure, patients undergoing coronary artery bypass grafting (CABG), implantable pacemakers or defibrillators, and patients with arrhythmias and claustrophobia. The study was approved by the local Ethics Committee. All patients provided written informed consent.

Cardiac MRI protocol

Cardiac MRI was performed on the Siemens 3 T whole-body MRI system (MAGNETOM Verio, A Tim System; Siemens Healthcare, Erlangen, Germany). A 32-element matrix coil was activated for data collection, and all sequences were electrocardiogram (ECG) gated. Total scan duration was approximately 1 hour. All images were acquired using phased array surface coils during mild expiration and electrocardiographic triggering. Eight millimetre sections with no intersection gap were acquired in the short-axis plane (from the base to the apex) and long-axis plane of the left ventricle to perform cine cardiac MRI and late gadolinium enhancement (LGE) imaging. LGE imaging was performed 15 minutes after the intravenous administration of gadolinium (Magnevist, Bayer Healthcare, 0.2 mmol/kg) by using a two-dimensional phase-sensitive inversion recovery breath-hold sequence (parameters: 2.4 ms repetition time [TR]/1.01 ms echo time [TE], 100 ms inversion time [TI], 12° flip angle; 8 mm section thickness; 99×160 matrix; 2.7×2.3 mm^2 in-plane spatial resolution; 651 Hz per pixel bandwidth). This acquisition was completed in ≥10 minutes (but no longer than 30 minutes) after the last administration of gadolinium.

Nuclear medicine protocol

Image acquisition was performed with fixed angle 90° dual-head single-photon-emission computed tomography (SPECT)/computed tomography (CT) camera (Precedence 16, Philips, Amsterdam, Netherlands) equipped with low-energy high-resolution collimator. The heart was included in the effective field of vision. Resting myocardial perfusion imaging was performed with ^{99m}Tc-MIBI (925 MBq, China Atomic Hi-Tech, Beijing, China) and 20% window at 140 keV. Collecting over 6×10^4 myocardial count level, image reconstruction was used by Astonish iterative method and Hanning filtering function, the cut-off frequency 0.62, order 10, iteration 4 times, subset number 8, without attenuation correction. ^{99m}Tc-MIBI was injected intravenously and image was presented after 1–1.5 hours. The patient is supine, the acquisition mode is step-by-shot, the acquisition parameters: matrix 128×128, 16-bit, magnification 1.5, rotation[18] 0 ° (32 frames, 25 seconds/frame). At each frame, eight ECG-gated frames according to per cardiac cycle were collected.

Myocardial 18F-fluorodeoxyglucose, digital superscript (^{18}F-FDG) imaging was performed within 2 days of ^{99m}Tc-MIBI imaging. After an overnight fast for at least 12 hours, an oral glucose of 25–50 g was given to the patients according to their serum glucose level. In diabetes patients, acipimox was administrated (500 mg, oral dose) before glucose loading. Insulin was administrated intravenously if the blood glucose level was >9 mmol/l at 45 minutes after oral glucose administration with close monitoring of blood glucose. When the blood glucose level was appropriate, ^{18}F-FDG (3 MBq/kg) was administered intravenously. PET images were acquired using PET/CT (Biograph mCT, Siemens, Pennsylvania, USA) equipped with a 52-ring PET that could accept 511 KeV peak collimator and 128 slice spiral CT. The heart was included in the effective field of vision and myocardial glucose metabolism imaging was performed using ^{18}F-FDG at a rotation of 360° (32 frames, 25 s/frame). The TrueX + time of flight (TOF) ultra-HD iteration method was used for short-axis reconstruction of the original image with two iterations, 21 subsets, image size 200, zoom 1.0, and Gaussian filter wave half height 8. Filtered back projection was performed using a Butterworth filter (cut-off frequency 0.17 cycles per pixel, order 8). The spatial resolution of the PET image was 2 mm. Eight ECG-gated frames per cardiac cycle were collected.

Segmental analysis

The left ventricle was divided into six basal, six mid-ventricular, four apical segments, and the apex using the

17-segmental model of the ACC/AHA.[13] The basal, mid-ventricular, and apical segments were analysed in the short-axis plane, the apex of the cardiac MRI image was analysed in the two-chamber long-axis plane, and the apex of the PET image was analysed in the horizontal and vertical long-axis plane. The myocardial regions supplied by the left anterior descending (LAD), left circumflex (LCX), and right coronary arteries (RCA) were selected according to the ACC/AHA criteria.[13,14]

Cardiac MRI image analysis

Cardiac MRI image analysis was undertaken using a Siemens workstation. All short-axis sections were projected on the two-chamber long-axis images and assigned to different positions according to their relationship with the papillary muscles. The mid-ventricular segments corresponded to the papillary muscle and the basal and apical segments corresponded to above and below the papillary muscle.[13] Visual analysis of each myocardial segment was performed and the wall motion of each myocardial segment was scored as follows: 1 (normal), 2 (hypokinesia), 3 (akinesia), and 4 (dyskinesia). The wall motion score index (WMSI) was calculated by dividing the sum of the coronary artery wall motion scores by the corresponding number of myocardial segments.[13]

All short-axis images of the left ventricle from the base to the apex were analysed. The transmural extent of myocardial infarction or scarring was analysed by LGE, which was defined as the percentage of delayed myocardial thickness to total myocardial thickness and was scored as 1 (0%), 2 (1–25%), 3 (26–50%), 4 (51–75%), and 5 (76–100%). LGE $\leq$50% was considered to indicate a viable myocardium.[15]

PET image analysis

PET data analysis was performed using Cedars software. Myocardium with normal blood perfusion and normal or increased ^{18}F-FDG uptake (normal) and myocardium with reduced blood perfusion but normal or increased ^{18}F-FDG uptake (mismatch) was considered to be viable myocardium. Myocardium with reduced blood perfusion and reduced ^{18}F-FDG uptake (match) was considered to be non-viable myocardium.

Cardiac MRI and PET data were analysed by two experienced radiologists and two experienced nuclear medicine physicians, respectively, who were blinded to each patient's clinical condition and the decision was made in consensus.

Global and regional left ventricular function analysis

Left ventricular volume, mass, ejection fraction (EF), end-diastolic volume (EDV), and end-systolic volume (ESV) were calculated from cardiac MRI short-axis images.

Statistical analysis

Data are expressed as mean ± standard deviation. Continuous data were compared using Student's *t* test or one-way analysis of variance. Continuous data of non-normal distribution were analysed using the Kruskal–Wallis test. Categorical variables were analysed using the chi-square test. Spearman's correlation analysis was used to analyse the correlation between different modalities, and Kappa analysis was used to compare the global agreement between different modalities. PET was used as the reference standard to calculate the sensitivity and specificity of cardiac MRI in detecting myocardial viability and the receiver operator characteristic (ROC) curve was used to analyse cardiac MRI performance for assessing myocardial viability. A p-value of <0.05 was considered to be statistically significant. All statistical analyses were performed using SPSS 23.

Results

In the present study, 1,360 myocardial segments were analysed in 80 patients. PET and cardiac MRI were performed in all patients within 1 week and there was no significant clinical change in any patient between the two examinations. The mean age of the patients was 56.9±10.2 years with 68 (85%) male patients. Detailed patient clinical characteristics are shown in Table 1.

Cardiac MRI and PET

There were 767 myocardial segments with LGE of 0%, 223 with LGE of 1–25%, 135 with LGE of 26–50%, 120 with LGE of 51–75%, and 115 with LGE of 76–100%. There were 892 normal myocardial segments, 260 mismatched myocardial segments, and 208 matched myocardial segments. Of the 892 normal myocardial segments, 20 (2.2%) had LGE >50%, of the 260 mismatched myocardial segments, 228 (87.7%)

Table 1
Basic patient characteristics.

Characteristics	Data
Sex	
Male	68 (85%)
Female	12 (15%)
Age (years)	
Mean±SD	56.9±10.2
Range	35–78
Previous infarction	25 (31.3%)
Smoke	45 (56.3%)
Hypertension	48 (60%)
Diabetes	18 (22.5%)
Hyperlipidaemia	25 (31.3%)
History of PCI	29 (36.3%)
CTO lesions	
LAD CTO	32 (34.4%)
LCX CTO	18 (19.4%)
RCA CTO	43 (46.2%)
Cardiac MRI parameters (Mean±SD)	
Ejection fraction (%)	53.5±15.1
End diastolic volume (ml)	121.8±65.3
End diastolic volume (ml)	55.7±40.9
Stroke volume (ml)	56.2±21.0
Myocardial mass (g)	118.5±48.7

SD, standard deviation; CTO, chronic total occlusion; MRI, magnetic resonance imaging; PCI, percutaneous coronary intervention; LAD, left anterior descending artery; LCX, left circumflex; RCA, right coronary artery.

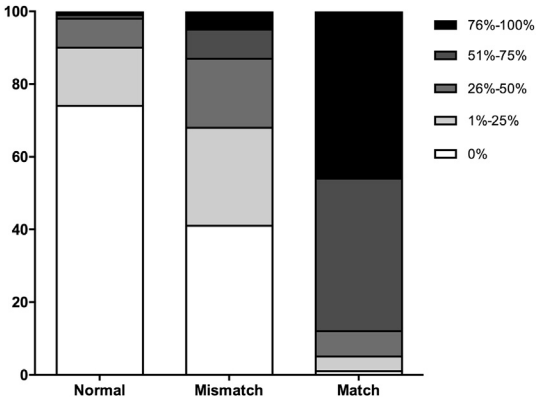

Figure 1 Distribution of LGE of myocardial segments in different types of myocardial viability determined by PET.

had LGE ≤50% and 32 (12.3%) had LGE>50%, and of the 208 matched myocardial segments, 25 (12%) had LGE ≤50% (Fig 1). PET examination of normal, mismatched, and matched myocardial segments with corresponding cardiac MRI examination results are shown in Figs 2–4. As shown in Table 2, there was a negative correlation between myocardial viability determined by PET and cardiac MRI-LGE ($p<0.001$; Table 2, Fig 5).

Comparison of cardiac MRI and PET in assessing myocardial viability on a per-patient basis

With PET as the reference standard, the sensitivity of cardiac MRI in assessing myocardial viability was 95.3%, specificity was 87.5%, positive predictive value was 96.8%, negative predictive value was 82.4%, and accuracy was 93.8% (Table 3). Furthermore, with PET as the reference standard for detection of myocardial viability, the ROC curve

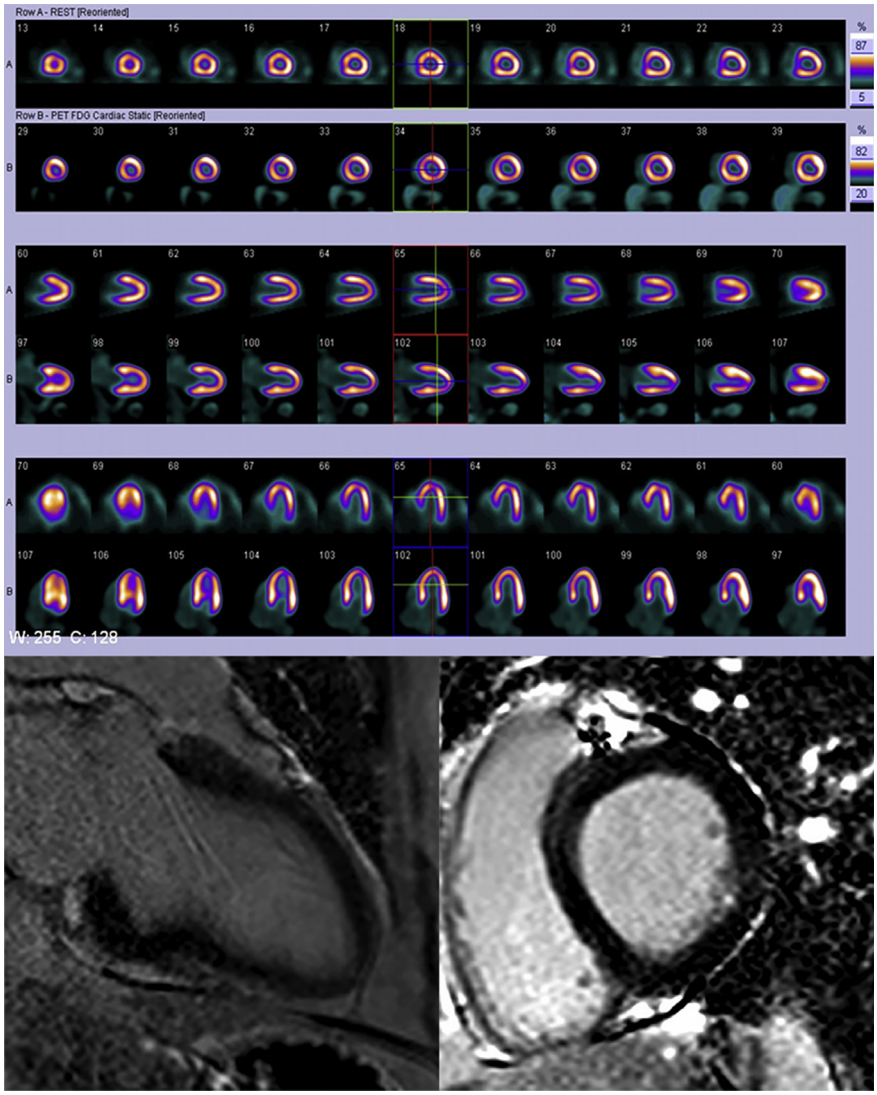

Figure 2 In a patient with chronic total occlusion of LCX, short axis, horizontal long axis, and vertical long axis SPECT perfusion (top row) and ^{18}F-FDG PET (bottom row) images were normal in all myocardial segments (normal) and short axis and vertical long axis cardiac MRI images showed that the LGE of corresponding myocardial segments was 0%.

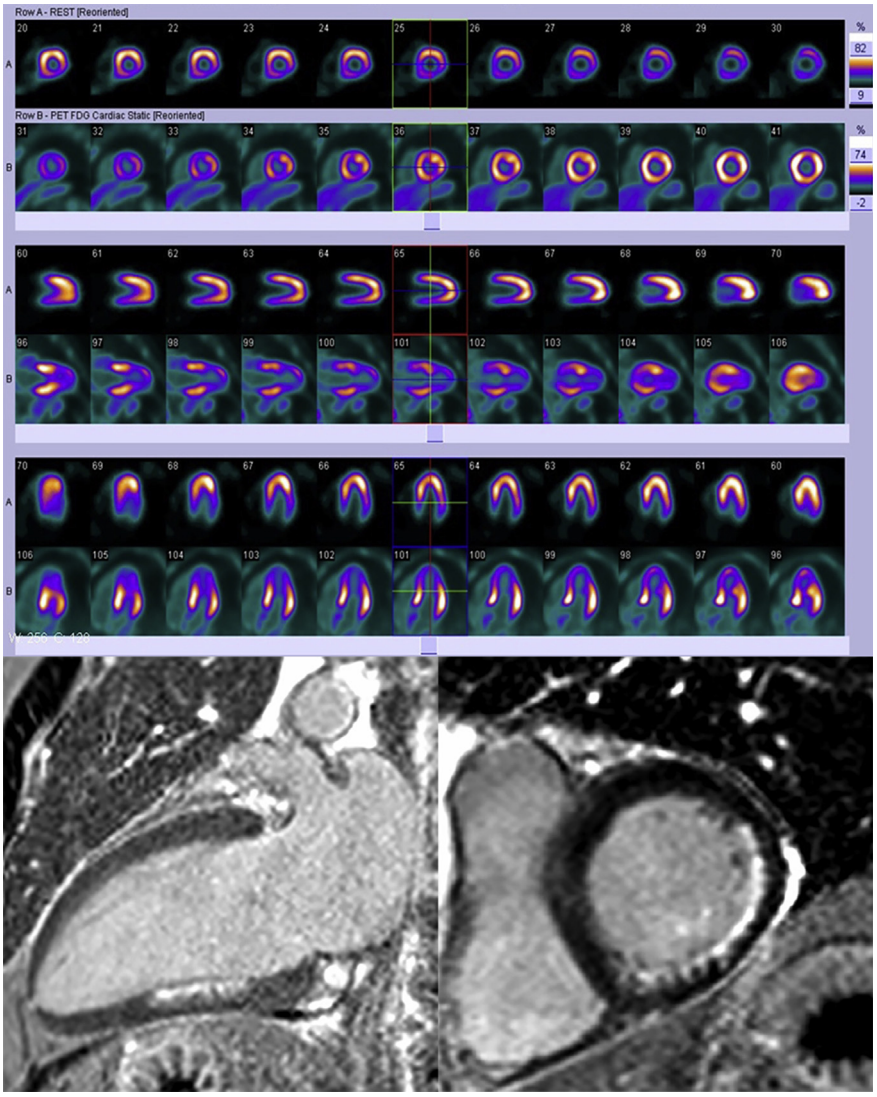

Figure 3 In a patient with chronic total occlusion of the right coronary artery, short axis and vertical long axis SPECT perfusion (top row) images showed a defect from the inferior wall to the posterolateral wall, and short axis and vertical long axis ^{18}F-FDG PET (bottom row) images showed a mild hypometabolism in corresponding myocardial segments (mismatched), short axis and vertical long axis cardiac MRI images showed that LGE of corresponding myocardial segments was 1–25%.

was used to analyse the performance of cardiac MRI for detection of myocardial viability (Fig 6) and the AUC was 0.910 (95% confidence interval 0.805 to 1). A threshold of 50% LGE was confirmed to yield optimal sensitivity and specificity for the differentiation of viable and non-viable myocardial segments defined by PET on a per-patient basis.

Comparison of cardiac MRI and PET in assessing myocardial motion

The motion of each myocardial segment was analysed using cardiac MRI and PET. The consistency and correlation of the two methods were analysed and the kappa value was 0.788 (r=0.825; p<0.001). According to the score of LGE, all myocardial segments were divided into five groups and the WMSI of each group was 1.13±0.28, 1.23±0.34, 1.56±0.35, 1.87±0.30 and 1.89±0.57 (p<0.0001; Fig 7). The WMSI of normal, mismatched, and matched group was 1.22±0.35, 1.40±0.40, and 2.21±0.58 (p<0.0001; Fig 8).

Discussion

Recently, studies have found that myocardial perfusion, systolic function, and prognosis of the corresponding myocardium in coronary CTO can be significantly improved after revascularization.[16,17] Gerber *et al.* and Allman *et al.* showed that patients with viable myocardium treated with revascularization had a better prognosis than those treated with conservative drug therapy. Furthermore, in patients without viable myocardium regardless of treatment, the prognosis was worse compared to patients with viable myocardium.[18,19] Kim *et al.* found that increased delayed enhancement indicated decreased possibility of functional recovery of abnormal myocardial segments after

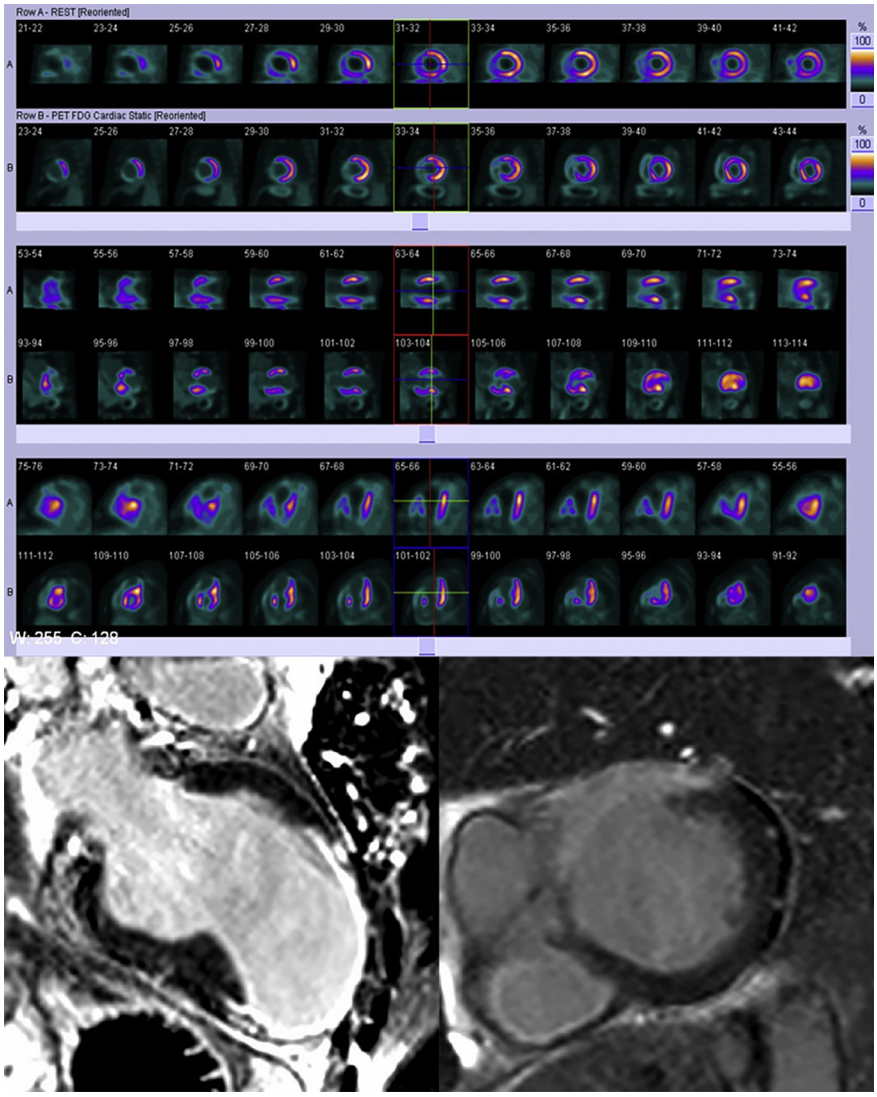

Figure 4 In a patient with chronic total occlusion of the LAD artery, short axis, horizontal long axis, and vertical long axis SPECT perfusion (top row) and ^{18}F-FDG PET (bottom row) images showed the apex, all myocardial segments of the apical and septal wall had severe defects (matched) and short axis and vertical long axis cardiac MRI images showed that LGE of corresponding myocardial segments was 76–100%.

Table 2
The relationship between LGE and PET in detecting viability of myocardial segments (n=1360).

PET	LGE				
	0%	1–25%	26–50%	51–75%	76–100%
Viable (n=1152)	765 (66.4%)	215 (18.7%)	120 (10.4%)	32 (2.8%)	20 (1.7%)
Non-viable (n=208)	3 (1.4%)	8 (3.9%)	16 (7.7%)	86 (41.3%)	95 (45.7%)

MRI, magnetic resonance imaging; LGE, late gadolinium enhancement; PET, positron emission tomography.

revascularization.[20] Therefore, evaluating the status and changes of myocardial viability before and after the opening of coronary arteries is very important for the long-term prognosis.

A total of 31 patients with ischaemic heart failure (EF=28%±9%) were enrolled in a study comparing myocardial viability with cardiac MRI and PET. The sensitivity and specificity in detecting viability using cardiac MRI compared to PET were 83% and 88%, respectively. In the normal myocardial segments as determined by PET, 11% showed delayed enhancement and in the matched myocardial segments as determined by PET, 5% of the myocardial segments showed no delayed enhancement.[9] In the present study, the sensitivity and specificity of cardiac MRI in detecting myocardial viability was 95.3% and 87.5%, respectively. In the normal myocardial segments as determined by PET, 27% showed delayed enhancement and in the matched myocardial segments as determined by PET, 1%

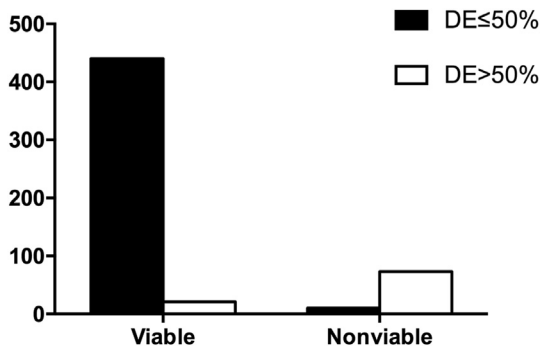

Figure 5 LGE of myocardial segments was classified according to myocardial viability as determined by PET.

Table 3
Analysis of myocardial viability by cardiac MRI and PET on a per patient basis (n=80).

PET	Cardiac MRI-LGE				
	0%	1–25%	26–50%	51–75%	76–100%
Normal (n=39)	18 (46.2%)	11 (28.2%)	8 (20.5%)	2 (5.1%)	0 (0%)
Mismatched (n=25)	11 (44%)	8 (32%)	5 (20%)	1 (4%)	0 (0%)
Matched (n=16)	0 (0%)	1 (6.2%)	1 (6.2%)	5 (31.3%)	9 (56.3%)

MRI, magnetic resonance imaging; LGE, late gadolinium enhancement; PET, positron-emission tomography.

showed no delay in enhancement. The specificity of the two studies was highly consistent but the sensitivity was different. The reason may be that the sample size of this study was relatively large and the number of myocardial segments with LGE >50% was relatively large in the viable segments as determined by PET.

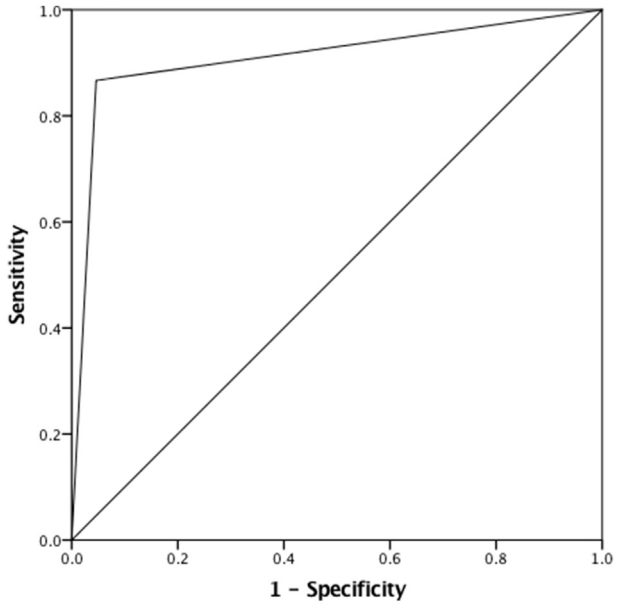

Figure 6 ROC curve analysis of the performance of cardiac MRI in detecting myocardial viability and the area under the curve was 0.910 (95% CI: 0.805 to 1).

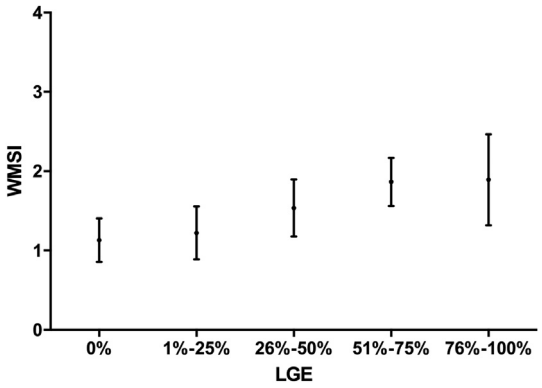

Figure 7 WMSI of myocardial segments classified by LGE.

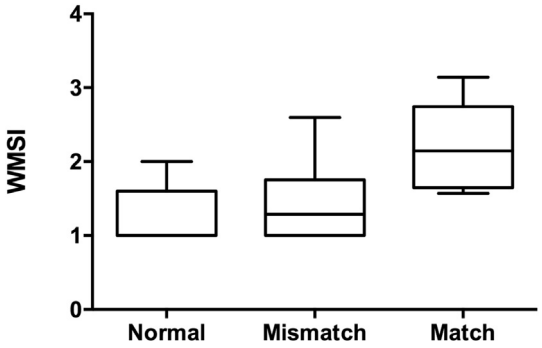

Figure 8 WMSI of myocardial segments classified by myocardial viability.

Kühl*et al.* showed that FDG uptake on PET had a very strong negative correlation with the degree of delayed enhancement on cardiac MRI (r=−0.86, p<0.001).[10] In that study, the performance of cardiac MRI was analysed by ROC curve and AUC was 0.95, the sensitivity and specificity of cardiac MRI in detecting myocardial viability was 96% and 84%. The results of the present study are highly consistent with their results. The optimal cut-off value of that study for LGE optimally differentiating viable from non-viable myocardium was 37%, but the result of the present study was 50%. The LGE ≤50% diagnostic criterion for viability at MRI was derived from a previous study[14] and confirmed after ROC analysis in the present study. The precise agreement concurs with the use of the pre-defined LGE range categories throughout, rather than a specific percentage LGE measurement for each patient. This will go some way to explaining the disparity between the previously published LGE cut-off of 37% in one study and the current finding of 50%. As 37% is roughly mid-way between the 25% and 50% cut-offs, the result is broadly in keeping with the previously published figure. The optimal cut-off value of the present study may have increased the number of viable myocardium as detected by cardiac MRI, resulting in the slightly higher specificity. The result of the optimal cut-off value in our study was consistent with the study of Kirschbaum.[21]

WMSI increased with increasing LGE, and there was a significant positive correlation between WMSI and LGE

($p<0.001$).[22] In a previous study, WMSI of the corresponding myocardial segment of CTO was higher compared to the myocardial segment corresponding of non-CTO and WMSI was higher in the myocardial segment with high LGE compared to the myocardial segment with low LGE.[23] In the present study, WMSI was highest in the group with an LGE of 76–100% and WMSI was lowest in the group with an LGE of 0%. It was concluded that WMSI was positively correlated with LGE, consistent with previous studies.

Due to differences in spatial resolution, cardiac MRI proved to be superior compared to nuclear imaging in the detection of small scars. Wagner *et al.* showed that the transmural infarction segments defined by the cardiac MRI could be detected by SPECT, but in 181 subendocardial infarction segments, 85 segments were not detected by SPECT.[24] Another study also showed that cardiac MRI had a better sensitivity in detecting myocardial infarction due to the higher spatial resolution.[25] Cardiac MRI can also provide overall and local cardiac function, myocardial perfusion, tissue characteristics, and other information in a single examination.[26] Therefore, the clinical application of cardiac MRI in evaluating myocardial viability is more promising.

The limitations of this study include the following aspects. Analysis of myocardial systolic function by low-dose dobutamine stress cardiac MRI may improve the diagnostic accuracy of myocardial function recovery after revascularization.[27] WMSI in the present study was calculated based on the entire myocardium dominated by each vessel and was not specific to each myocardial segment. Some studies have analysed the changes of left ventricular function after revascularization,[28–30] and further analysis of the changes in left ventricular function is needed in future studies. In addition, large-scale randomized controlled studies are needed to confirm the necessity of evaluating myocardial viability before interventional treatment of coronary CTO lesions.[28]

In conclusion, cardiac MRI assessment of myocardial viability in patients with coronary CTO has very good consistency and high accuracy compared to PET. Therefore, cardiac MRI can be used as a very important method to evaluate myocardial viability in patients with coronary CTO and it has important clinical significance for treatment choice in patients with coronary CTO.

Conflict of interest

There are no conflicts of interest.

Acknowledgements

This study was supported by the Beijing Municipal Science and Technology Project (no. Z161100000516139), Beijing Lisheng Cardiovascular Health Foundation Pilot Fund Project (no. LHJJ20158521), Translational Medicine Project of Dalian Medical University (no. 2015003), Beijing Lab for Cardiovascular Precision Medicine (no. PXM2017_014226_000037) and National Natural Science Foundation (no. 81671650). This study is part of the registration trial (ClinicalTrials.gov NCT02767401).

References

1. Sianos G, Werner GS, Galassi AR, *et al*. Recanalisation of chronic total coronary occlusions: 2012 consensus document from theEuroCTO club. *EuroIntervention* 2012;**8**(1):139–45.
2. Stone GW, Kandzari DE, Mehran R, *et al*. Percutaneous recanalization of chronically occluded coronary arteries: a consensus document: part I. *Circulation* 2005;**112**(15):2364–72.
3. Zidar FJ, Kaplan BM, O'Neill WW, *et al*. Prospective, randomized trial of prolonged intracoronary urokinase infusion for chronic total occlusions in native coronary arteries. *J Am Coll Cardiol* 1996;**27**(6):1406–12.
4. Christofferson RD, Lehmann KG, Martin GV, *et al*. Effect of chronic total coronary occlusion on treatment strategy. *Am J Cardiol* 2005;**95**(9):1088–91.
5. Galassi AR, Tomasello SD, Reifart N, *et al*. In-hospital outcomes of percutaneous coronary intervention in patients with chronic total occlusion: insights from the ERCTO (European Registry of Chronic Total Occlusion) registry. *EuroIntervention* 2011;**7**(4):472–9.
6. Levine GN, Bates ER, Blankenship JC, *et al*. 2011 ACCF/AHA/SCAI guideline for percutaneous coronary intervention: a report of the American College of Cardiology Foundation/American Heart Association task force on practice guidelines and the society for cardiovascular angiography and interventions. *Circulation* 2011;**124**(23):574–651.
7. Windecker S, Kolh P, Alfonso F, *et al*. 2014 ESC/EACTS guidelines on myocardial revascularization: the task force on myocardial revascularization of the european society of Cardiology (ESC) and the european association for cardio-thoracic surgery (EACTS) developed with the special contribution of the european association of percutaneous cardiovascular interventions (EAPCI). *Eur Heart J* 2014;**35**(37):2541–619.
8. Allman KC. Noninvasive assessment myocardial viability: current status and future directions. *J Nucl Cardiol* 2013;**20**(4):618–37.
9. Klein C, Nekolla SG, Bengel FM, *et al*. Assessment of myocardial viability with contrast-enhanced magnetic resonance imaging imaging: comparison with positron emission tomography. *Circulation* 2002;**105**(2):162–7.
10. Kühl HP, Beek AM, van der Weerdt AP, *et al*. Myocardial viability in chronic ischemic heart disease: comparison of contrast-enhanced magnetic resonance imaging imaging with (18)F-fluorodeoxyglucose positron emission tomography. *J Am Coll Cardiol* 2003;**41**(8):1341–8.
11. Wu YW, Tadamura E, Yamamuro M, *et al*. Comparison of contrast-enhanced MRI with (18)F-FDG PET/201Tl SPECT in dysfunctional myocardium: relation to early functional outcome after surgical revascularization in chronic ischemic heart disease. *J Nucl Med* 2007;**48**(7):1096–103.
12. Roes SD, Kaandorp TA, Marsan NA, *et al*. Agreement and disagreement between contrast-enhanced magnetic resonance imaging imaging and nuclear imaging for assessment of myocardial viability. *Eur J Nucl Med Mol Imaging* 2009;**36**(4):594–601.
13. Cerqueira MD, Weissman NJ, Dilsizian V, *et al*. Standardized myocardial segmentation and nomenclature for tomographic imaging of the heart: a statement for healthcare professionals from the Cardiac Imaging Committee of the Council on Clinical Cardiology of the American Heart Association. *Circulation* 2002;**105**(4):539–42.
14. Pereztol-Valdés O, Candell-Riera J, Santana-Boado C, *et al*. Correspondence between left ventricular 17 myocardial segments and coronary arteries. *Eur Heart J* 2005;**26**(24):2637–43.
15. Kim RJ, Fieno DS, Parrish TB, *et al*. Relationship of MRI delayed contrast enhancement to irreversible injury, infarct age, and contractile function. *Circulation* 1999;**100**(19):1992–2002.
16. Pujadas S, Martin V, Rosselló X, *et al*. Improvement of myocardial function and perfusion after successful percutaneous revascularization in patients with chronic total coronary occlusion. *Int J Cardiol* 2013;**169**(2):147–52.
17. Olivari Z, Rubartelli P, Piscione F, *et al*. Immediate results and one-year clinical outcome after percutaneous coronary interventions in chronic total occlusions: data from a multicenter, prospective, observational study (TOAST-GISE). *J Am Coll Cardiol* 2003;**41**(10):1672–8.
18. Gerber BL, Rousseau MF, Ahn SA, *et al*. Prognostic value of myocardial viability by delayed-enhanced magnetic resonance imaging in patients

with coronary artery disease and low ejection fraction: impact of revascularization therapy. *J Am Coll Cardiol* 2012;**59**(9):825–35.
19. Allman KC, Shaw LJ, Hachamovitch R, *et al*. Myocardial viability testing and impact of revascularization on prognosis in patients with coronary artery disease and left ventricular dysfunction: a meta-analysis. *J Am Coll Cardiol* 2002;**39**(7):1151–8.
20. Kim RJ, Wu E, Rafael A, *et al*. The use of contrast-enhanced magnetic resonance imaging imaging to identify reversible myocardial dysfunction. *N Engl J Med* 2000;**343**(20):1445–53.
21. Kirschbaum SW, Rossi A, Boersma E, *et al*. Combining magnetic resonance imaging viability variables better predicts improvement of myocardial function prior to percutaneous coronary intervention. *Int J Cardiol* 2012;**159**(3):192–7.
22. Ripley DP, Gosling OE, Bhatia L, *et al*. The relationship between the contralateral collateral supply and myocardial viability on cardiovascular magnetic resonance imaging: can the angiogram predict functional recovery? *Int J Cardiol* 2014;**177**(2):362–7.
23. Choi JH, Chang SA, Choi JO, *et al*. Frequency of myocardial infarction and its relationship to angiographic collateral flow in territories supplied by chronically occluded coronary arteries. *Circulation* 2013;**127**(6):703–9.
24. Wagner A, Mahrholdt H, Holly TA, *et al*. Contrast-enhanced MRI and routine single photon emission computed tomography (SPECT) perfusion imaging for detection of subendocardial myocardial infarcts: an imaging study. *Lancet* 2003;**361**(9355):374–9.
25. Ordovas KG, Higgins CB. Delayed contrast enhancement on MRI images of myocardium: past, present, future. *Radiology* 2011;**261**(2):358–74.
26. Saeed M, Hetts SW, Do L, *et al*. MRI study on volume effects of coronary emboli on myocardial function, perfusion and viability. *Int J Cardiol* 2013;**165**(1):93–9.
27. Baer FM, Theissen P, Schneider CA, *et al*. Dobutamine magnetic resonance imaging imaging predicts contractile recovery of chronically dysfunctional myocardium after successful revascularization. *J Am Coll Cardiol* 1998;**31**(5):1040–8.
28. Baks T, van Geuns RJ, Duncker DJ, *et al*. Prediction of left ventricular function after drug-eluting stent implantation for chronic total coronary occlusions. *J Am Coll Cardiol* 2006;**47**(4):721–5.
29. Kühl HP, Lipke CS, Krombach GA, *et al*. Assessment of reversible myocardial dysfunction in chronic ischaemic heart disease: comparison of contrast-enhanced cardiovascular magnetic resonance and a combined positron emission tomography-single photon emission computed tomography imaging protocol. *Eur Heart J* 2006;**27**(7):846–53.
30. Kirschbaum SW, Baks T, van den Ent M, *et al*. Evaluation of left ventricular function three years after percutaneous recanalization of chronic total coronary occlusions. *Am J Cardiol* 2008;**101**(2):179–85.